



NRC Publications Archive Archives des publications du CNRC

Correlation between Young's Modulus and Impregnation Quality of Epoxy-Impregnated SWCNT Buckypaper

Ashrafi, Behnam; Guan, Jingwen; Mirjalili, Vahid; Hubert, Pascal; Simard, Benoit; Johnston, Andrew

This publication could be one of several versions: author's original, accepted manuscript or the publisher's version. / La version de cette publication peut être l'une des suivantes : la version prépublication de l'auteur, la version acceptée du manuscrit ou la version de l'éditeur.

For the publisher's version, please access the DOI link below. / Pour consulter la version de l'éditeur, utilisez le lien DOI ci-dessous.

Publisher's version / Version de l'éditeur:

<https://doi.org/10.1016/j.compositesa.2010.04.018>

Composites Part A : Applied Science and Manufacturing, 41, 9, pp. 1184-1191, 2010-04-26

NRC Publications Record / Notice d'Archives des publications de CNRC:

<https://nrc-publications.canada.ca/eng/view/object/?id=7c91208f-2de7-4abb-9314-1e58bf4a305a>

<https://publications-cnrc.canada.ca/fra/voir/objet/?id=7c91208f-2de7-4abb-9314-1e58bf4a305a>

Access and use of this website and the material on it are subject to the Terms and Conditions set forth at

<https://nrc-publications.canada.ca/eng/copyright>

READ THESE TERMS AND CONDITIONS CAREFULLY BEFORE USING THIS WEBSITE.

L'accès à ce site Web et l'utilisation de son contenu sont assujettis aux conditions présentées dans le site

<https://publications-cnrc.canada.ca/fra/droits>

LISEZ CES CONDITIONS ATTENTIVEMENT AVANT D'UTILISER CE SITE WEB.

Questions? Contact the NRC Publications Archive team at

PublicationsArchive-ArchivesPublications@nrc-cnrc.gc.ca. If you wish to email the authors directly, please see the first page of the publication for their contact information.

Vous avez des questions? Nous pouvons vous aider. Pour communiquer directement avec un auteur, consultez la première page de la revue dans laquelle son article a été publié afin de trouver ses coordonnées. Si vous n'arrivez pas à les repérer, communiquez avec nous à PublicationsArchive-ArchivesPublications@nrc-cnrc.gc.ca.





Correlation between Young's modulus and impregnation quality of epoxy-impregnated SWCNT buckypaper

Behnam Ashrafi^{a,b}, Jingwen Guan^c, Vahid Mirjalili^b, Pascal Hubert^{b,*}, Benoit Simard^c, Andrew Johnston^a

^a Structures and Material Performance Laboratory, Institute for Aerospace Research, National Research Council of Canada, Ottawa, Ontario, Canada K1A 0R6

^b McGill University, Department of Mechanical Engineering, 817 Sherbrooke Street West, Montreal, QC, Canada H3A 2K6

^c Molecular and Nanomaterial Architectures Group, Steacie Institute for Molecular Sciences, National Research Council of Canada, Ottawa, Ontario, Canada K1A 0R6

ARTICLE INFO

Article history:

Received 8 December 2009

Received in revised form 23 April 2010

Accepted 26 April 2010

Keywords:

- A. Nano-structures
- B. Elasticity
- B. Porosity
- C. Micro-mechanics

ABSTRACT

Carbon nanotube (CNT) sheets, also known as buckypaper, have high potential for structural applications due to their high volume fraction of CNT, the strongest and stiffest materials known. In this work, two different techniques, one based on positive pressure and another based on vacuum infiltration, are utilized to impregnate single-walled carbon nanotube (SWCNT) buckypaper sheets of 50–70 μm in thickness, resulting in a Young's modulus of up to 15.4 GPa. Scanning electron microscopy demonstrates that the vacuum-based technique results in more effective impregnation of the buckypaper than the positive pressure technique. Thermogravimetry analysis of vacuum-impregnated specimens indicated a void content ranging from 5% to 32%. An advanced Mori–Tanaka-based micromechanics technique is also utilized to predict the effect of SWCNT volume fraction and void content on Young's modulus of nanocomposites. These calculations suggest a higher void content of around 40% for the vacuum-impregnated composites.

© 2010 Elsevier Ltd. All rights reserved.

1. Introduction

Buckypaper sheets are typically formed by vacuum filtration of a suspended solution of randomly distributed carbon nanotubes (CNT). Buckypaper is appropriate for a wide range of applications including electrodes [1], gas separators [2], field emitters [3], actuators [4], and sensors [5]. Buckypaper sheets are also good candidates for polymer reinforcement for structural applications due to their high CNT content (up to 60% by weight after impregnation). Hence, several researchers have investigated the elastic properties of pristine buckypaper sheets [1,4,6–9] and their composites [8–15]. The measured Young's modulus of pristine buckypaper has been shown to range from 0.8 to 5 GPa. This property was found to be dependent on the type and treatment of the CNT [7] and the humidity content [1]. Table 1 summarizes experimental results found in the literature for the elastic properties of pristine buckypaper. These results are comparable to theoretical values predicted with the classical Cox model [16]. The effect of the CNT rope properties (diameter, length, and Young's modulus) and sheet porosity on buckypaper Young's modulus were also thoroughly investigated in [17]. Another theoretical model was developed to predict the upper-bound moduli of buckypaper containing nanotube ropes with an emphasis on the effect of joint

morphology [7]. The predicted buckypaper Young's modulus ranged from 1% to 10% of the bundle Young's modulus. This suggests the possibility of a 2- to 15-fold increase in buckypaper Young's modulus (versus the best experimental data) if the area (volume) fraction and the connection numbers between CNT ropes were increased.

Several researchers have tried to manufacture buckypaper composites using different techniques such as through-thickness infiltration [11,12], intercalation [8,9], electro-spinning [13], and hot-compression [10]. Also, different types of polymers were used including epoxy [11], polycarbonate (PC) [12,15], polyvinyl alcohol (PVA), poly vinyl pyrrolidone (PVP) and poly styrene (PS) [8,9], poly-ether-ether-ketone (PEEK) [10] and different elastomers [13]. A summary of the elastic properties of buckypaper composites with randomly oriented single-walled carbon nanotubes (SWCNT) or multi-walled carbon nanotube (MWCNT) is tabulated in Table 2. Typically, the Young's modulus of buckypaper nanocomposites is measured by dynamic mechanical analysis [11,12], quasi-static tests using dynamic mechanical analyzers [8–10,13] and tensile tests using dog-bone specimens [14]. A recent study [14] measured a Young's modulus of 30 GPa for epoxy-impregnated buckypaper composites. This value can be attributed to a higher quality of impregnation as well as a higher content (40–45% by weight) of CNT than other buckypaper composites reported in the literature (Table 2). In another recent study, Cheng et al. [18] reported a Young's modulus of up to 47 GPa after the impregnation

* Corresponding author.

E-mail address: pascal.hubert@mcgill.ca (P. Hubert).

Table 1
Elastic properties of pristine buckypaper.

Ref.	E_{BP} (GPa)	Type of CNT
[6]	0.8–5.0	SWCNT
[1]	0.3–2.2	SWCNT
[7]	1.1–4	SWCNT
[4]	1.2	SWCNT
[9]	2.3	SWCNT
[8]	0.9	SWCNT
[18]	1.1	MWCNT

of randomly distributed buckypaper using bismaleimide resin as well as 169 GPa after the impregnation of mechanically stretched buckypaper sheets. This high value of Young's modulus is likely due to CNT alignment and high CNT content (60% by weight) as well as a low void content.

Wide variation in the reported Young's modulus of buckypaper nanocomposites (Table 2) can be attributed to several factors including the level of impregnation, the quality and content of CNT within the buckypaper as well as the quality of the interface between the CNT and the matrix resin. Therefore, the results presented in Table 2 are not conclusive for evaluation of the merits of different manufacturing techniques. In this work, two different impregnation techniques, vacuum infiltration and hot-compression, were used to impregnate thin sheets (50–70 μm thick) of buckypaper sheets. A scanning electron microscope (SEM) was used for qualitative evaluation of the impregnation techniques. Bending tests and thermogravimetric analysis (TGA) were utilized to obtain the Young's modulus and void content of impregnated buckypaper sheets, respectively. Experimental results were compared with theoretical predictions based on a Mori–Tanaka technique.

Table 2
Elastic properties of buckypaper nanocomposites.

Ref.	E_{BP}^a (GPa)	CNT content	Polymer	E_p^a (GPa)	Impregnation method	E_c^a (GPa)	E_c/E_{BP}	E_c/E_{BP}
[13]	–	–	Silicone elastomer	0.20	Spin coating	0.42	–	2.1
[9]	2.3	27–41 vol.%	PVA, PS, PVP	–	Intercalation	6.9	3	–
[8]	0.9	27–41 vol.%	PVP	–	Intercalation	3.2	3.5	–
[10]	–	–	PEEK	2.7	Hot-compression	8	–	3
[11]	–	28–39 wt.%	Epoxy	2.8	Resin infiltration	13.3	–	4.7
[14]	–	40–45 wt.%	Epoxy	2.8	Intercalation and hot-compression	30	–	10.7
[18]	1.1	60 wt.%	Bismale-imide	–	Intercalation and hot-compression	47	42.7	–
[12]	–	20 wt.%	PC	1.8	Vacuum infiltration	6.2	–	3.4
[15]	2.29	46–48 wt.%	PC	1.7	Vacuum infiltration	3	1.3	1.8

^a BP, P, and C stand for buckypaper, polymer and composite, respectively.

2. Composite manufacturing

2.1. Buckypaper manufacturing

In this work, raw SWCNT samples manufactured using our two-laser oven technique [19,20] were subjected to a purification procedure involving cycles of solvent extraction, floatation and precipitation. The recovery of purified SWCNT was 30–50% by weight, with a purity of more than 90% by weight [26]. Dried and purified SWCNT samples (roughly 800 mg) were ground in a small amount of tetrahydrofuran (THF) with a mortar. The fine paste was then transferred to a 2 L beaker with 1.5 L of ethanol or methanol. The mixture was sonicated with a sonication probe for about an hour until a well dispersed suspension was attained. Using a water pump, the suspension was filtered through a polycarbonate (PC) membrane with a pore size of $>20 \mu\text{m}$ and a diameter of 47 mm. As soon as the solvent was drained, the water pump was stopped. The wet buckypaper, together with the membrane, was placed between two sheets of wax paper and pressed overnight between two metal cylinder blocks under a force equivalent to 10 MPa. After pressing, the PC membrane was carefully removed. Finally, the pristine buckypaper was dried in an oven overnight at 85 $^{\circ}\text{C}$.

TGA tests were performed to characterize the purity of the pristine buckypaper. A residue of 8–10% of the buckypaper weight was measured after reaching 1000 $^{\circ}\text{C}$ in an oxygen environment, at which point no CNT remained. The residue was composed of metal oxides (around 3% of the buckypaper weight) and small particles of quartz glass. This represents only those impurities that remained following the heating process; additional impurities would have been burned off at temperatures below 1000 $^{\circ}\text{C}$. A Hitachi S-4700 field emission scanning electron microscope (FESEM) was also utilized to characterize the pristine buckypaper. Fig. 1 shows

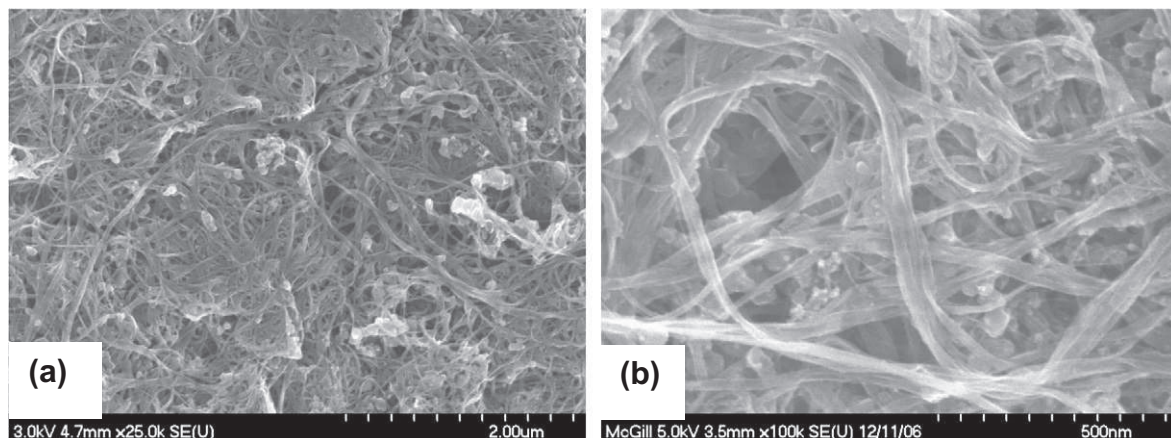


Fig. 1. SEM images of pure buckypaper with (a) 25 K and (b) 100 K magnifications.

Table 3
Properties of buckypaper.

Property	Value
Thickness	50–70 ^a
Area	13–19 cm ²
Impurity content by weight	>10%
SWCNT diameter	~1.3 nm
SWCNT rope diameter	10–50 nm
SWCNT rope aspect ratio	>1000
Density	0.46–0.55 g/cm ³
SWCNT rope volume fraction	25–35 (%)
Young's modulus	0.5 ± 0.2

^a Thickness variation of each film was ±1 μm.

images of pristine buckypaper with SWCNT rope diameters ranging from 10 nm to 50 nm and the presence of impurities.

An average buckypaper density of 0.55 g/cm³ was calculated from measurements of buckypaper weight, thickness and surface area. Assuming a density of 1.3 g/cm³ for SWCNT ropes [21] and a minimum of 10% impurities, an average SWCNT rope volume fraction of 30% was measured for the buckypaper. This volume fraction agrees well with buckypaper CNT volume fractions reported by other researchers (Table 2). Table 3 summarizes the measured properties of the pristine buckypaper developed in this work.

2.2. Impregnation techniques

Two different techniques were employed to impregnate the SWCNT buckypaper, as described below.

2.2.1. Vacuum infiltration technique

The first technique used was a vacuum infiltration technique which is schematically illustrated in Fig. 2. Using this method, a vacuum pressure of 28 in Hg (98.4 kPa) was applied to the system to infiltrate the buckypaper with Araldite[®] MY0510 epoxy resin supplied by Huntsman. 4,4-Diaminodiphenyl Sulphone (DDS) was used as the hardener. A breather material was used to evacuate the air from the buckypaper. A porous release film was inserted between the buckypaper and the breather in order to separate the buckypaper composite from the breather after impregnation. An amount of resin sufficient for complete impregnation was placed

over the buckypaper using a stirring rod. A thin layer of vacuum tape was placed around the edges of the buckypaper to prevent the resin from escaping.

A TA instruments AR2000 Rheometer with an Environmental Test Chamber (ETC) accessory was used to measure the viscosity of the MY0510 epoxy resin and hardener as a function of time for four different temperatures (60, 100, 120, and 140 °C). The viscosity was found to be roughly 10 Pa s at room temperature, decreasing to about 0.1 Pa s at 100 °C. It was found that infiltration at 100 °C was the best option since this gave a sufficiently low viscosity which was relatively constant over a period of over 3 h, which was long enough for the infiltration process.

In accordance with Darcy's law for one-dimensional flow, the infiltration time (t) is given by [12]:

$$t = \frac{\eta h^2}{2K_f \Delta P} \quad (1)$$

Here, η is the viscosity of the resin, h is the sheet thickness, ΔP is the vacuum pressure, and K_f is the permeability of the sheet.

Wang et al. [11] obtained a permeability (K_f) of 2×10^{-19} m² through the thickness of a similar buckypaper sheet, assumed to be a good first approximation for the permeability of the buckypaper used in this work. Using this value, an impregnation time of around 2.5 h was calculated as being required to impregnate our buckypaper sheets, assuming a typical thickness of 60 μm, a vacuum pressure of 98.4 kPa, and a resin viscosity of 0.1 Pa s. To ensure sufficient time for infiltration, vacuum was maintained for an additional period of 3 h at 100 °C followed by a final cure at 177 °C for 2 h.

2.2.2. Hot-compression technique

The second infiltration technique employed was a hot-compression method using a hot press. Using this approach, a sufficient amount of resin was first poured over the SWCNT buckypaper within a cavity defined by an O-ring which prevented excess leakage. Steel shims were used to control the thickness (Fig. 3). The two plates of the hot press were placed in contact with each other with light pressure, and then heated to 100 °C. This temperature was maintained while a force equivalent to a pressure of 40 MPa was applied to the system for a period of 3 h. The buckypaper composite was then cured in situ at a temperature of 177 °C for a period of 2 h.

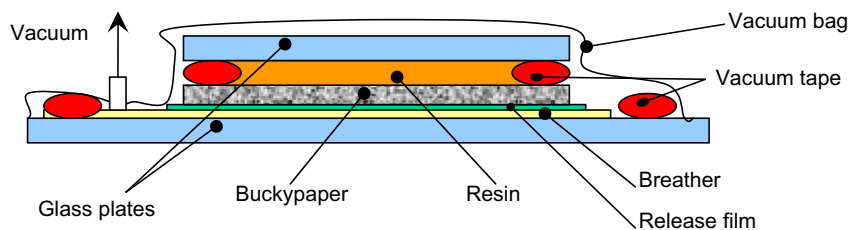


Fig. 2. Schematic illustration of the vacuum infiltration technique used for impregnation of the buckypaper.

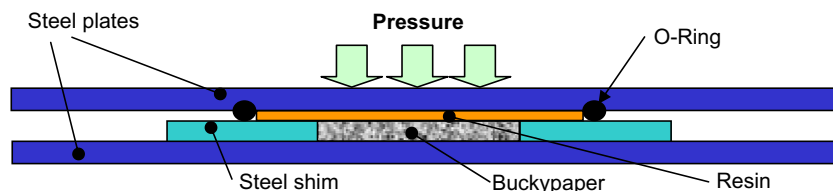


Fig. 3. Schematic illustration of the hot-compression technique for impregnation of buckypaper.

3. Qualitative characterization of buckypaper

Fig. 4 shows a cross-sectional view of a vacuum-infiltrated film. Comparing the images of pristine and impregnated buckypaper, a very different morphology indicative of the infiltration of resin into the buckypaper (Fig. 4a) can be observed. The presence of small air bubbles is also clear in the higher magnification images (Fig. 4b). Fig. 5 shows SEM images of samples manufactured by the hot-compression technique. Two distinct regions can be observed (Fig. 5a); a resin-rich region and a non-impregnated region. Under pressure, the resin is forced to penetrate the buckypaper, but due to its extremely low permeability, this resin displaced the ropes, creating channels through the buckypaper with lateral dimensions of a few micrometers. It is also speculated that air trapped between the two steel substrates and the O-ring (Fig. 3) may inhibit efficient infiltration. Fig. 5b shows a magnified view at the boundary of the two regions that suggests that the resin wets the CNT ropes well in this area. However, Fig. 5c indicates an absence of resin in most regions of the buckypaper. Recall that this was not the case for the vacuum infiltration technique in which the vacuum was applied more uniformly to the resin, resulting in a more uniform impregnation of the buckypaper.

4. Elastic characterization of SWCNT buckypaper

A nanoindenter-based bending technique described in [22] was used to obtain the elastic properties of pristine buckypaper, neat epoxy and resin-impregnated buckypaper nanocomposite sheets. In this method, bending tests are performed on clamped circular

plates to measure the Young's modulus of thin sheets. This approach combines the micronewton and nanometer resolution of a typical nanoindenter with the conceptual simplicity of a bending test [22]. A maximum load of 1 mN was applied using the nanoindenter at a loading rate of 1 mN/s. This rate is the highest possible for this instrument (Hysitron Triboindenter) and was chosen to minimize viscoelastic effects. All sheets had thicknesses between 50 μm and 70 μm with a thickness variation of less than 1 μm across individual sheets. Table 4 summarized the results of pristine and impregnated buckypaper sheets as well as pure epoxy specimens. The bending tests on pure polymer sheets lead to an average value of 3.5 GPa, which compares well with the value indicated by the resin manufacturer (3.4 GPa), demonstrating the accuracy of the technique.

5. Impregnation quantitative evaluation

To evaluate the resin and void content of the buckypaper composites, TGA tests were performed on pure polymer, pristine buckypaper and thin nanocomposite sheets using a Netzsch TG 209 F1 Iris[®]. The system was operated with BOC UHP argon (5.3) gas and residual oxygen was captured with a Supelco Big-Supel-pure O oxygen/water trap. Tests were carried out from room temperature to 600 °C with a heating rate of 10 °C/min. Two 20 min holds were added to the temperature cycle at 450 °C and 600 °C to obtain an accurate weight measurement of the residue from each specimen at these two temperatures. Two to three tests were performed on each sample (Fig. 6 shows the average for each sample). The variations between different tests on each specimen were

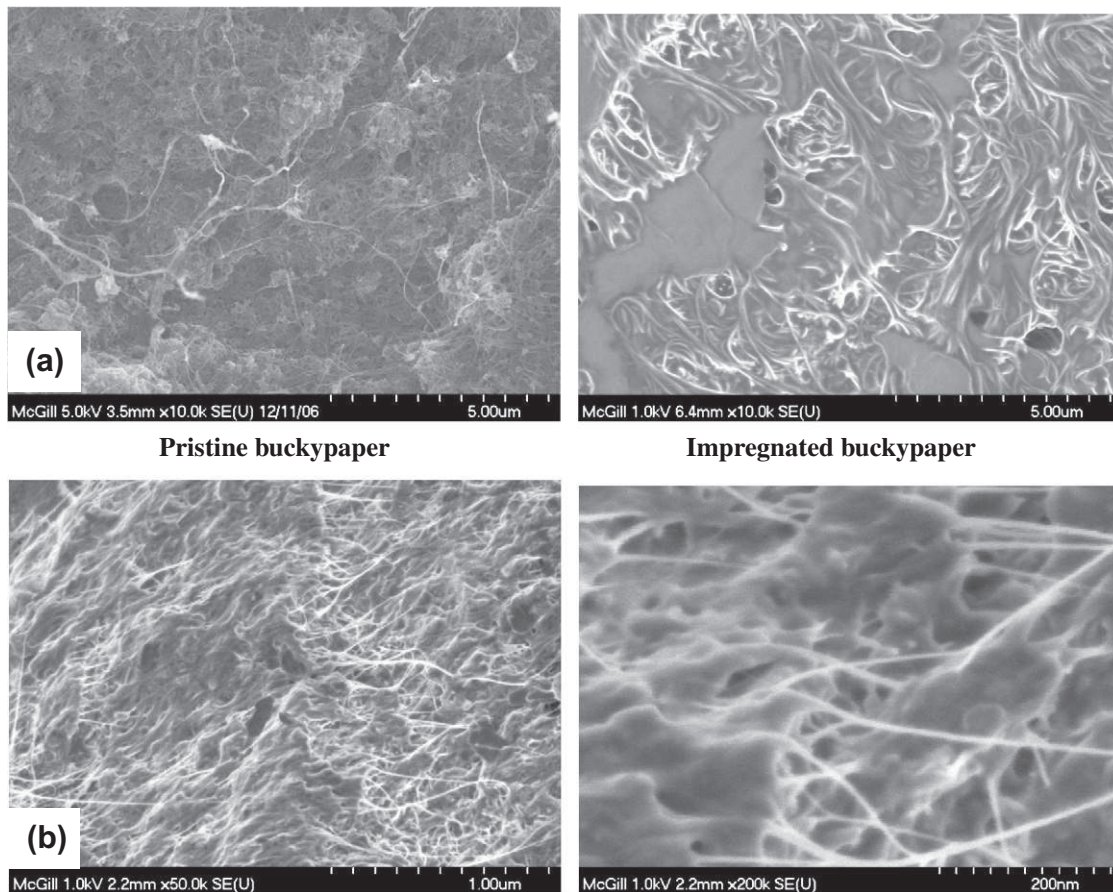


Fig. 4. Cross-sectional view of vacuum-infiltrated samples. (a) A comparison between pristine buckypaper and impregnated buckypaper. (b) A fractured surface with magnifications of 50 K and 200 K showing good impregnation of SWCNT buckypaper.

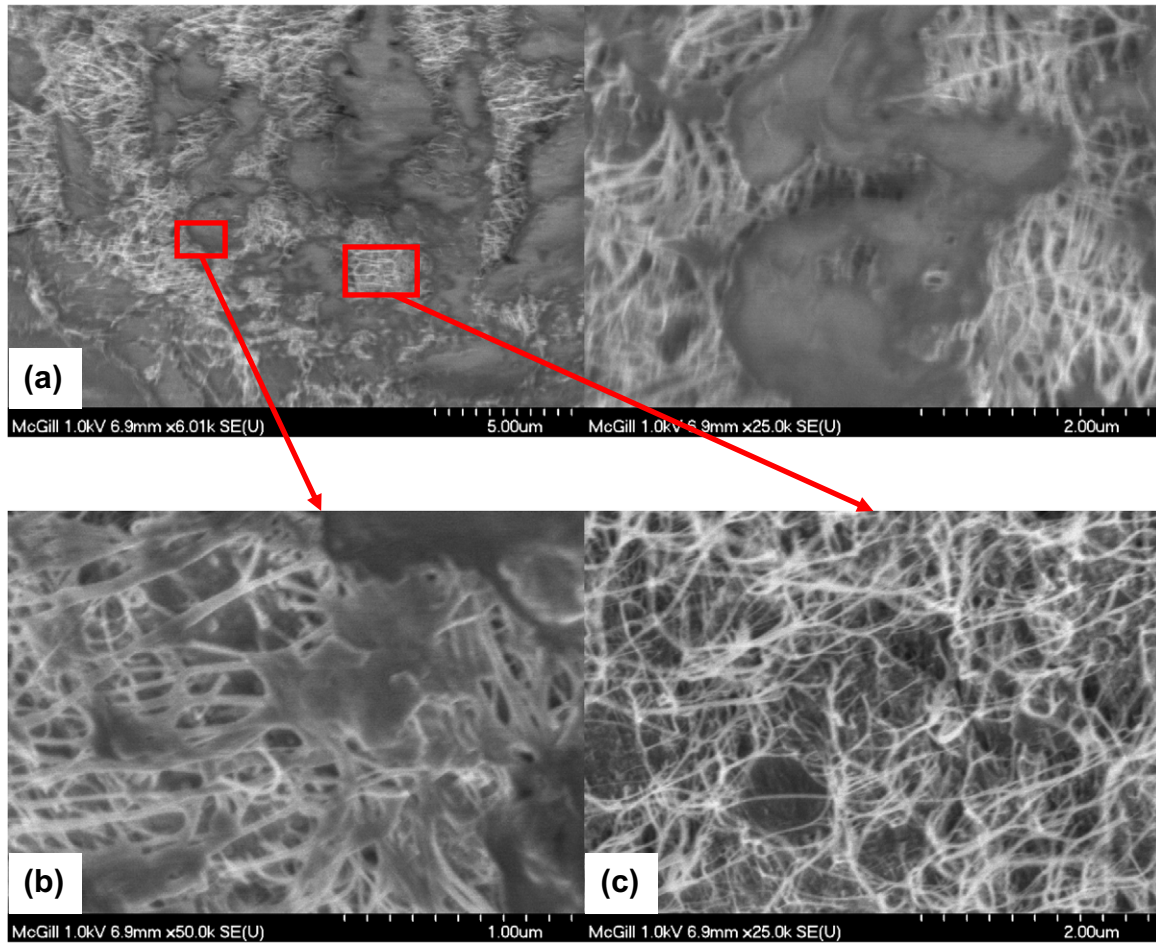


Fig. 5. Cross-sectional view of hot-compression samples. (a) Two distinct regions can be differentiated: a resin-rich region and a non-impregnated region. (b) Good resin wetting can be observed at the boundary of these two regions. (c) Middle of CNT-rich region, showing no sign of resin infiltration.

Table 4
Young's modulus of buckypaper, polymer and nanocomposite sheets (all values are GPa).

Sample	Neat epoxy	Pristine buckypaper	Nanocomposite (vacuum-infiltrated)	Nanocomposite (hot-compression)
Sample 1	3.8	0.58	6.4	4.1
Sample 2	3.5	0.74	15.4	3.1
Sample 3	3.5	0.40	7.3	3.8
Sample 4	3.4	0.30	14.5	2.9
Average	3.5 ± 0.2	0.50 ± 0.20	11.0 ± 4.7	3.5 ± 0.5

very small (less than 3% by weight). To evaluate weight fractions of polymer matrix ($w_{f,M}$) and carbon nanotube ropes ($w_{f,F}$) within the buckypaper, we have:

$$1 = w_{f,F} + w_{f,M} + w_{f,I} \quad (\text{room temperature}) \quad (2)$$

$$m_C = m_F w_{f,F} + m_M w_{f,M} + w_{f,I} \quad (\text{elevated temperatures}) \quad (3)$$

where m_F , m_M , and m_C are the weight residue of carbon nanotubes, polymer matrix and the nanocomposite, respectively, obtained from the TGA results, and $w_{f,I}$ is the weight content of impurities and is equal to 9% based on the results presented in Section 2.1. This percentage remains constant during the TGA heat treatments.

From Eqs. (2) and (3), the resin weight fraction is calculated from Eq. (4):

$$w_{f,R} = \frac{m_F - m_C + w_{f,I}(1 - m_F)}{m_F - m_R} \quad (4)$$

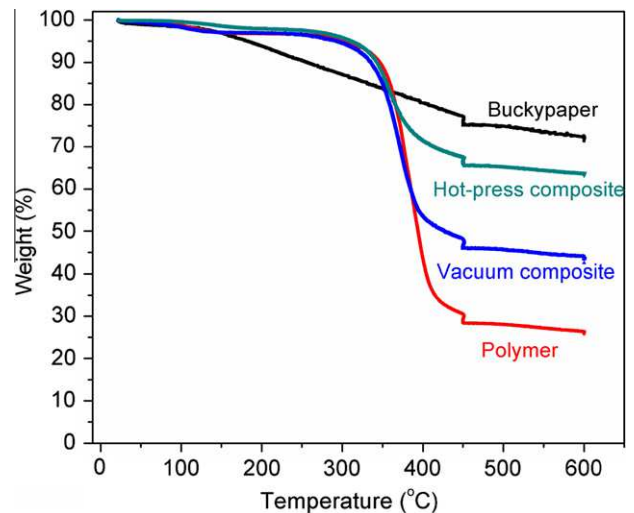


Fig. 6. TGA of polymer, buckypaper and thin nanocomposite sheets (hot-compression and vacuum-infiltrated). Tests performed with argon purge gas at a heating rate of 10 °C/min with two 20 min holds at 450 °C and 600 °C.

From the TGA results shown in Fig. 6, buckypaper composites show the same weight loss trend as the neat resin system below 350 °C, which indicates resin decomposition only. However, above this temperature, the trends and amounts of weight losses of each

specimen become significantly different before weight losses stabilized at about 450 °C. Also, the larger weight reduction of pristine buckypaper at lower temperatures can be attributed to the moisture content. Another possible reason could be due the presence of thermally less stable, smaller diameter SWCNT within the buckypaper. Also can be seen from Fig. 6, a weight residue of about 25% was measured for neat epoxy at temperatures above 450 °C, which seems to be higher than the typical weight residue of most epoxies. This higher weight residue can be due to the thermal decomposition rather than burning of the epoxy as all TGA tests were performed in an inert environment using argon purge gas. Another possibility for this higher residue can be due to the fact that the epoxy used in this work is specifically designed for high temperature applications. From Eq. (4), the weight fraction of resin inside the vacuum-infiltrated nanocomposites was measured from the residual weights at 450 °C to be about 66%. However, the weight fraction of resin within the nanocomposites manufactured by hot-compression was only about 25%, confirming that this technique was not as effective as the vacuum method. The differences between the weight fractions calculated at representative temperatures between 450 °C and 600 °C were negligible, below 0.5% and 4.5% for vacuum and hot-compression manufactured composites, respectively.

In order to estimate void content, nanocomposite density (ρ_c) was evaluated from:

$$\rho_c = \frac{v_{f.F} \rho_F}{w_{f.F}} \quad (5)$$

where ρ_F is the SWCNT rope density (considered to be 1.3 g/cm³) and $v_{f.F}$ is the rope volume fraction, which varied between 25% and 35% (estimated for pristine buckypaper). Finally, the matrix

volume fraction ($v_{f.M}$) and void content (Vc) were obtained from Eqs. (6) and (7):

$$v_{f.M} = \rho_c / \rho_M - v_{f.F} \rho_F / \rho_M \quad (6)$$

$$Vc = 1 - v_{f.M} - v_{f.F} \quad (7)$$

where ρ_M is the epoxy density (taken to be 1.2 g/cm³). Due to the lack of information about the type and content of impurities within buckypaper, the weight of impurities was ignored in void content calculations.

Assuming a volume fraction of 25–35% for buckypaper SWCNT ropes, a void content of 5–32% and 54–66% was calculated for the vacuum-infiltrated and for hot-compression nanocomposites, respectively.

6. Micromechanical evaluation of modulus and void content

Theoretical bounds for the elastic properties of the SWCNT buckypaper composites were predicted using the Mori–Tanaka approach [23]. In the model the buckypaper composite was assumed to be composed of ellipsoidal SWCNT ropes randomly distributed throughout the matrix (Fig. 7a). SWCNT ropes were considered transversely isotropic with an aspect ratio of 1000 and an axial Young’s modulus of 580 GPa [24] (other elastic constants used for the modelling of the ropes can be found elsewhere, see [25]). A Young’s modulus of 3.5 GPa and a Poisson’s ratio of 0.4 were used for the epoxy matrix.

Fig. 8 shows a comparison of experimental results with Mori–Tanaka predictions for a range SWCNT volume fraction from 25% to 35%. These results suggest that a threefold increase in the elastic modulus of buckypaper composites is possible upon improvement in the quality of impregnation. To evaluate the effect of void con-

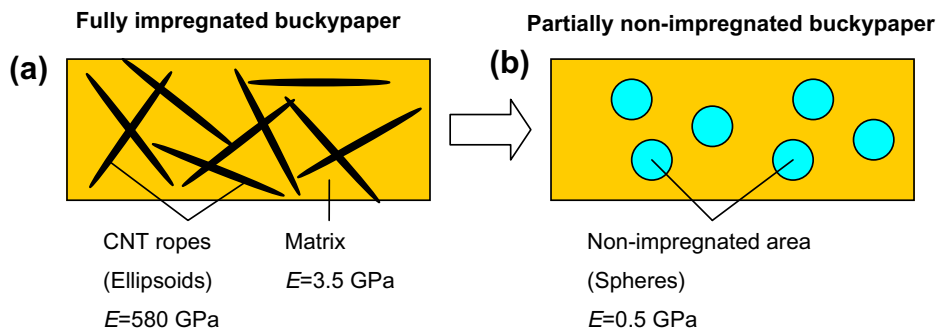


Fig. 7. Mori–Tanaka modelling of (a) fully impregnated nanocomposite and (b) a buckypaper composite with non-impregnated area represented by spheres.

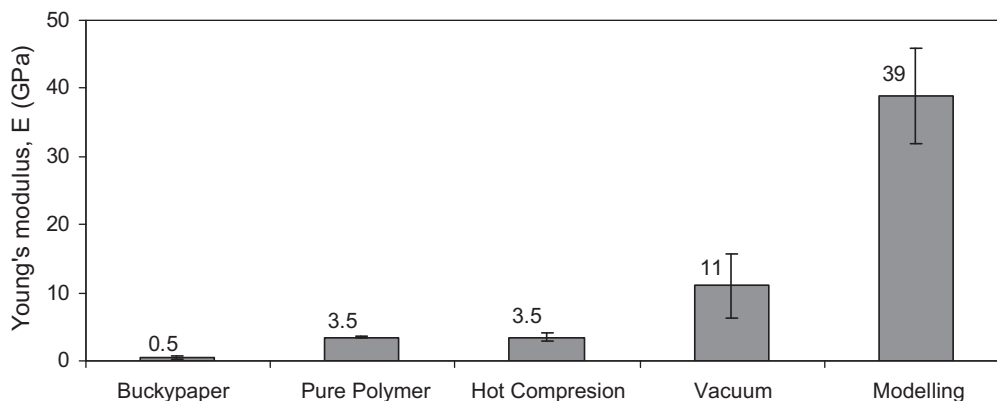


Fig. 8. A comparison between experimental measurements for different sheets (neat epoxy, pristine buckypaper and impregnated buckypaper) and predictions derived using a Mori–Tanaka technique for SWCNT rope volume fractions from 25% to 35%, assuming perfect impregnation.

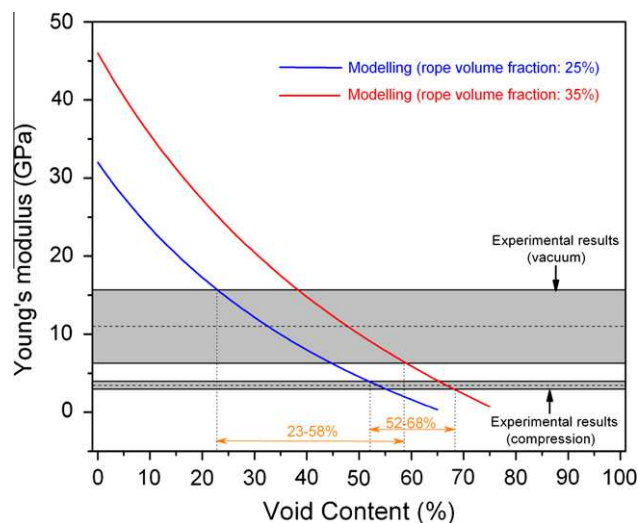


Fig. 9. Effect of void content on Young's modulus of buckypaper composites with SWCNT rope volume fractions of 25% and 35%. Bounds on Young's modulus of characterized nanocomposites are also shown.

Table 5

Buckypaper composite void contents obtained through TGA and Mori–Tanaka's approach.

	Hot-compression technique (%)	Vacuum-infiltration technique (%)
TGA measurement	55–68	3–31
Modelling	52–68	23–58

tent on Young's modulus, un-impregnated regions were modelled as spherical inclusions randomly distributed throughout the impregnated buckypaper composites (Fig. 7b). A Young's modulus of 0.5 GPa and Poisson's ratio of 0.3 were assigned to these inclusions.

Experimental measurements and model predictions for the Young's modulus of the buckypaper composites as a function of void content are shown in Fig. 9 and summarized in Table 5. For nanocomposites manufactured through the hot-compression technique, model predictions of void content compare well with experimental results. However, for vacuum-infiltrated buckypaper composites, the model predicts a higher void content than measured. Different factors can explain this difference. First, the Mori–Tanaka approach assumes perfect load transfer between resin and nanotubes, which would overestimate the elastic properties in cases when the bonding between resin and SWCNT ropes is poor. Second, in the theoretical calculations, a longitudinal Young's modulus of 580 GPa was assigned to the SWCNT ropes. This value is for ideal SWCNT ropes and obtained through molecular dynamics simulations [24]. In as-manufactured materials, however, the presence of defects and missing SWCNT inside ropes can result in degraded mechanical properties. Finally, SEM images show a considerable quantity of impurities inside the pristine buckypaper (Fig. 1), possibly higher than the amount of 10% assumed here. This will reduce the actual volume fraction of SWCNT ropes, resulting in a reduction of elastic properties.

7. Conclusions

Epoxy-impregnated buckypaper sheets manufactured through a vacuum infiltration technique produced nanocomposites with a Young's modulus of up to 15.4 GPa. This was comparable to the results obtained through other experimental work reported earlier in the literature (Table 2). However, due to different impregnation

techniques, different polymers used for impregnation, lack of information about the elastic properties of pristine buckypaper and the final buckypaper void content, a direct comparison between this work and others is not possible.

Theoretical results obtained through Mori–Tanaka approach suggest the possibility of a further increase of 3–4 times in the elastic properties of impregnated buckypaper (Fig. 8). Experimental and theoretical evaluations of nanocomposite void content clearly show that the impregnation process of buckypaper sheets was imperfect. Moreover, the presence of a relatively wide range of void content for vacuum-impregnated SWCNT buckypaper composites (5–32%) is also consistent with the relatively wide range of elastic Young's modulus for these composites (6.4–15.4 GPa).

Acknowledgements

Financial support from the Natural Sciences and Engineering Research Council (NSERC) of Canada through the Discovery Grants Program and a PGSD scholarship are gratefully acknowledged.

References

- [1] Whitten PG, Spinks GM, Wallace GG. Mechanical properties of carbon nanotube paper in ionic liquid and aqueous electrolytes. *Carbon* 2005;43(9):1891–6.
- [2] Cooper SM, Chuang HF, Cinke M, Cruden BA, Meyyappan M. Gas permeability of a buckypaper membrane. *Nano Lett* 2003;3(2):189–92.
- [3] Knapp W, Schleussner D. Field-emission characteristics of carbon buckypaper. *J Vacuum Sci Technol B: Microelectron Nanometer Struct* 2003;21(1 SPEC.):557–61.
- [4] Baughman RH, Cui C, Zakhidov AA, Iqbal Z, Barisci JN, Spinks GM, et al. Carbon nanotube actuators. *Science* 1999;284(5418):1340–4.
- [5] Dharap P, Li Z, Nagarajaiah S, Barrera EV. Nanotube film based on single-wall carbon nanotubes for strain sensing. *Nanotechnology* 2004;15(3):379–82.
- [6] Zhang X, Sreekumar TV, Liu T, Kumar S. Properties and structure of nitric acid oxidized single wall carbon nanotube films. *J Phys Chem B* 2004;108(42):16435–40.
- [7] Berhan L, Yi YB, Sastry AM, Munoz E, Selvidge M, Baughman R. Mechanical properties of nanotube sheets: alterations in joint morphology and achievable moduli in manufacturable materials. *J Appl Phys* 2004;95(8):4335–45.
- [8] Frizzell CJ, In Het Panhuis M, Coutinho DH, Balkus KJ, Minett AJ, Blau WJ, et al. Reinforcement of macroscopic carbon nanotube structures by polymer intercalation: the role of polymer molecular weight and chain conformation. *Phys Rev B – Condens Matter Phys* 2005;72(24):1–8.
- [9] Coleman JN, Blau WJ, Dalton AB, Munoz E, Collins S, Kim BG, et al. Improving the mechanical properties of single-walled carbon nanotube sheets by intercalation of polymeric adhesives. *Appl Phys Lett* 2003;82(11):1682–4.
- [10] Song L, Zhang H, Zhang Z, Xie S. Processing and performance improvements of SWNT paper reinforced peek nanocomposites. *Composites Part A* 2007;38(2):388–92.
- [11] Wang Z, Liang Z, Wang B, Zhang C, Kramer L. Processing and property investigation of single-walled carbon nanotube (swnt) buckypaper/epoxy resin matrix nanocomposites. *Composites Part A* 2004;35(10):1225–32.
- [12] Wang S, Liang Z, Pham G, Park YB, Wang B, Zhang C, et al. Controlled nanostructure and high loading of single-walled carbon nanotubes reinforced polycarbonate composite. *Nanotechnology* 2007;18(9).
- [13] Lahiff E, Leahy R, Coleman JN, Blau WJ. Physical properties of novel free-standing polymer-nanotube thin films. *Carbon* 2006;44(8):1525–9.
- [14] Jianwen Bao QC, Wang Xianping, Liang Richard, Zhang Chuck, Wang Ben, Kramer Leslie, et al. Functionalization of carbon nanotube sheets for high-performance composites applications. *SAMPE* 2009, Baltimore, Maryland; 2009.
- [15] Pham GT, Park Y-B, Wang S, Liang Z, Wang B, Zhang C. Mechanical and electrical properties of polycarbonate nanotube buckypaper composite sheets. *Nanotechnology* 2008;19(32):325705.
- [16] Cox HL. The elasticity and strength of paper and other fibrous materials. *Brit J Appl Phys* 1952;3(3):72–9.
- [17] Astrom JA, Krashennnikov AV, Nordlund K. Carbon nanotube mats and fibers with irradiation-improved mechanical characteristics: a theoretical model. *Phys Rev Lett* 2004;93(21).
- [18] Cheng Q, Bao J, Park J, Liang Z, Zhang C, Wang B. High mechanical performance composite conductor: multi-walled carbon nanotube sheet/bismaleimide nanocomposites. *Adv Funct Mater* 2009;19(20):3219–25.
- [19] Kingston CT, Simard B. Recent advances in laser synthesis of single-walled carbon nanotubes. *J Nanosci Nanotechnol* 2006;6(5):1225–32.
- [20] Kingston CT, Jakubek ZJ, Dénommée S, Simard B. Efficient laser synthesis of single-walled carbon nanotubes through laser heating of the condensing vaporization plume. *Carbon* 2004;42(8–9):1657–64.

- [21] Pipes RB, Frankland SJV, Hubert P, Saether E. Self-consistent properties of carbon nanotubes and hexagonal arrays as composite reinforcements. *Compos Sci Technol* 2003;63(10):1349–58.
- [22] Ashrafi B, Pronovost R, Hubert P, Vengallatore S. Elastic characterization of swnt-reinforced polymer thin films using a nanoindenter-based bending test. In: 49th AIAA/ASME/ASCE/AHS/ASC structures, structural dynamics, and materials conference, Schaumburg, IL, USA; 2008.
- [23] Mori T, Tanaka K. Average stress in matrix and average elastic energy of materials with misfitting inclusions. *Acta Metall* 1973;21(5):571–4.
- [24] Popov VN, Van Doren VE, Balkanski M. Elastic properties of crystals of single-walled carbon nanotubes. *Solid State Commun* 2000;114(7):395–9.
- [25] Ashrafi B, Hubert P, Vengallatore S. Carbon nanotube-reinforced composites as structural materials for microactuators in microelectromechanical systems. *Nanotechnology* 2006;17(19):4895–903.
- [26] Guan JW, Simard B. Unpublished results.